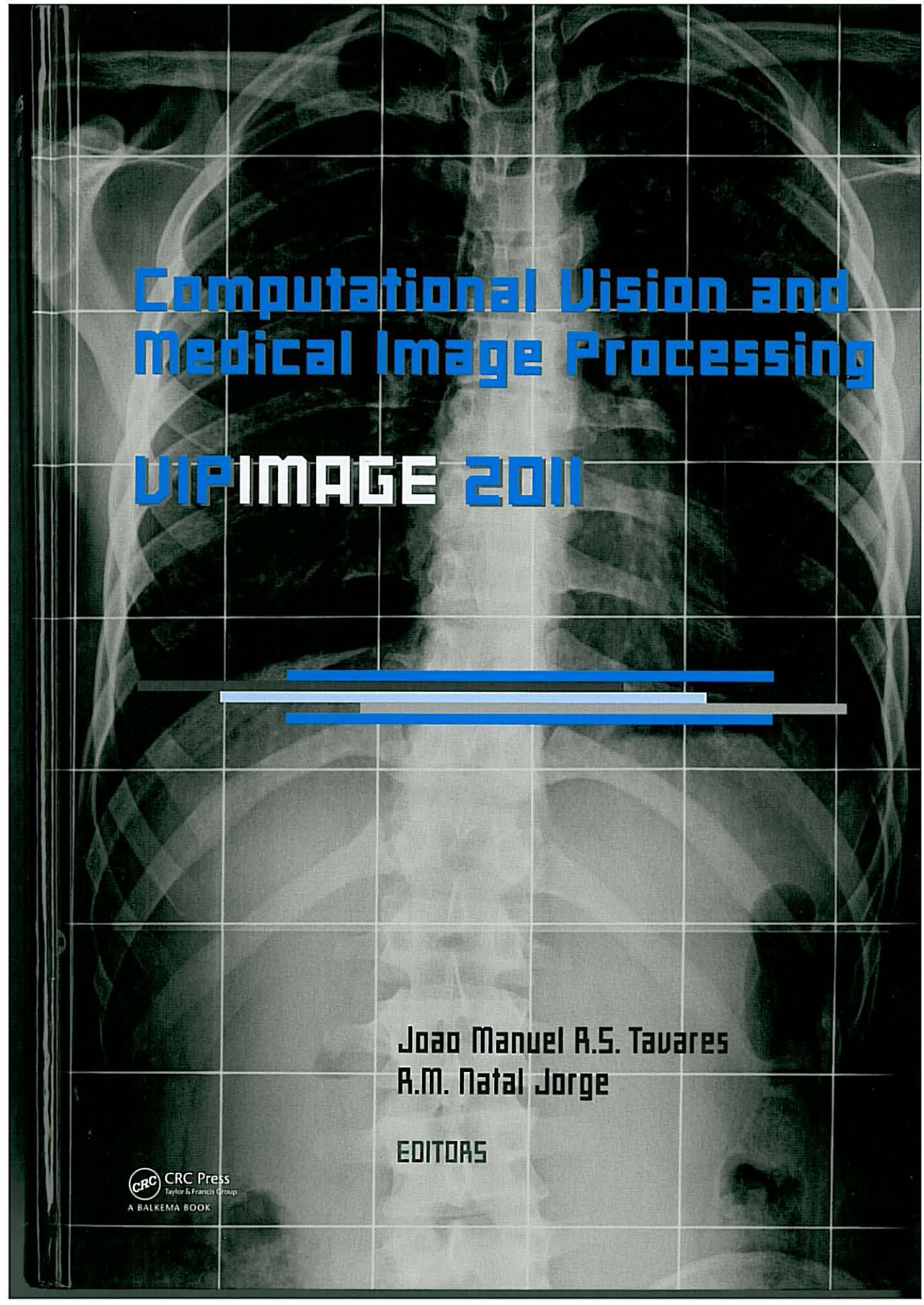

Computational Vision and Medical Image Processing

VIPIMAGE 2011

Joao Manuel R.S. Tavares
R.M. Natal Jorge

EDITORS

CRC Press
Taylor & Francis Group
A BALKEMA BOOK

CRC Press/Balkema is an imprint of the Taylor & Francis Group, an informa business

Typeset by Vikatan Publishing Solutions (P) Ltd., Chennai, India
Printed and bound by CPI Group (UK) Ltd, Croydon, CRO 4YY

Published by: CRC Press/Balkema
P.O. Box 447, 2300 AK Leiden, The Netherlands
e-mail: Pub.NL@taylorandfrancis.com
www.crcpress.com – www.taylorandfrancis.co.uk – www.balkema.nl

ISBN: 978-0-415-68395-1 (Hbk)
ISBN: 978-0-203-12818-3 (eBook)

PROCEEDINGS OF VIPIMAGE 2011 – THIRD ECCOMAS THEMATIC CONFERENCE ON COMPUTATIONAL VISION AND MEDICAL IMAGE PROCESSING, OLHÃO, ALGARVE, PORTUGAL, 12–14 OCTOBER 2011

Computational Vision and Medical Image Processing

VipIMAGE 2011

Editors

João Manuel R.S. Tavares & R.M. Natal Jorge

Faculdade de Engenharia da Universidade do Porto

Porto, Portugal

CRC Press

Taylor & Francis Group

Boca Raton London New York Leiden

CRC Press is an imprint of the

Taylor & Francis Group, an informa business

A BALKEMA BOOK

Computational Vision and Medical Image Processing – Tavares & Natal Jorge (eds)
© 2012 Taylor & Francis Group, London, ISBN 978-0-415-68395-1

Flow of Red Blood Cells through a microfluidic extensional device: An image analysis assessment

T. Yaginuma, A.I. Pereira & P.J. Rodrigues
ESTiG, IPB, C. Sta. Apolonia, Bragança, Portugal

R. Lima
ESTiG, IPB, C. Sta. Apolonia, Bragança, Portugal
CEFT, FEUP, R. Dr. Roberto Frias, Porto, Portugal

M.S.N. Oliveira
CEFT, FEUP, R. Dr. Roberto Frias, Porto, Portugal

T. Ishikawa
Department of Bioengineering and Robotics, Graduate School of Engineering, Tohoku University, Aoba, Sendai, Japan

T. Yamaguchi
Department of Biomedical Engineering, Graduate School of Engineering, Tohoku University, Aoba, Sendai, Japan

ABSTRACT: The present study aims to assess the deformability of Red Blood Cells (RBCs) under extensionally dominated microfluidic flows using an image based technique. For this purpose, a microchannel having a hyperbolic shaped-contraction was used and the images were captured by a standard high-speed microscopy system. The images acquired display RBCs with various light intensity levels and image analysis was used to quantify the Deformation Index (DI) of the RBCs considering these light intensity differences. Additionally, the velocities of different intensity-level RBCs flowing along the centerline of the channel were measured using particle tracking velocimetry. The preliminary results at two different flow rates reveal a highly deformable nature of RBCs when submitted to strong extensional flows. It was also observed that the low intensity cells exhibit a slightly higher velocity than intermediate intensity cells, which we attribute to the cells being located in different planes.

1 INTRODUCTION

Red Blood Cells (RBCs) are known as a highly deformable blood component that plays an important role in delivering oxygen to the tissues in microcirculation. According to Mokken et al. (1992) the capacity of RBCs to deform is related to three main characteristics: the viscoelastic properties of its membrane; the high surface area-to-volume ratio associated with its biconcave discoid shape; and the viscosity of its intracellular solution. A variation of any of these factors can have a significant impact on RBC deformability leading to serious health consequences. In particular a decrease in RBC deformability can result in impaired perfusion of the peripheral tissues. Furthermore, it has been reported that the elastic characteristics as well as the shape of RBCs are important factors to explain the etiology of certain pathologies (Mokken et al. 1992). As a consequence, there has been a number of studies on RBC deformability, which use, among others, techniques such as RBC filtration (Gueguen et al. 1984), laser diffraction ellipsometry (Shin et al. 2004) and rheoscopy (Dobbe et al. 2002). Most of these studies focus on the effect of shear flow. However, extensionally-dominated flows are often found in the human circulatory system, namely when there is a change in the cross-sectional area, e.g. in stenoses and in the transition from vessels to catheters (Selby et al. 2003, Fujiwara et al. 2009). In this study, we use an image analysis to characterize the velocity and deformation index of RBCs flowing through microchannels having a hyperbolic shape (Fig. 1). The shape of the channels was chosen so that the fluid at the centerline is submitted to a strong extensional flow and experiences a nearly constant strain rate (Oliveira et al. 2007).

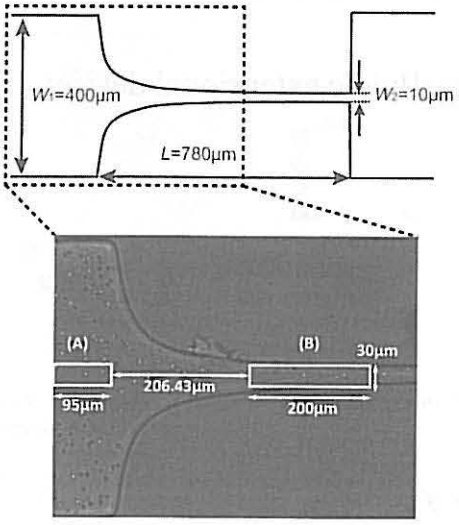

Figure 1. Geometry and dimensions of the PDMS hyperbolic microchannel.

Typically, the images captured by standard microscopy systems using a high speed camera display RBCs with various light intensity levels, but to the best of our knowledge, few studies have considered this difference in the analysis. Therefore, our investigation on RBC behavior is based on an image analysis performed considering the different RBC intensity levels. The results obtained for different flow rates indicate the highly deformable nature of RBCs under strong extensional flows.

2 MATERIALS AND METHODS

2.1 *Working fluids and microchannel geometry*

The working fluid examined was composed of Dextran 40 (Dx40) containing ~1% of human RBCs (i.e., hematocrit, Hct~1%). The blood used was collected from a healthy adult volunteer, and EDTA (ethylenediaminetetraacetic acid) was added to the collected samples to prevent coagulation. The blood samples were then submitted to washing and centrifuging processes and were then stored hermetically at 4°C until the experiments were performed at a temperature of ~37°C. All procedures were carried out in compliance with the guidelines of the Ethics Committee on Clinical Investigation of Tohoku University.

The microchannels containing the hyperbolic contraction were produced in polydimethylsiloxane (PDMS) using standard soft-lithography techniques from a SU-8 photoresist mold. The molds were prepared in a clean room facility by photo-lithography using a high-resolution chrome mask. The geometry and dimensions of the micro-fabricated channels are shown in Fig. 1. The channel depth, h, was constant throughout the PDMS chip and the width of the upstream and downstream channels was the same, $W_1 = 400$ μm. The minimum width in the contraction region is $W_2 = 10$ μm, defining a total Hencky strain of $\varepsilon_H = \ln(W_1/W_2) = \ln(40)$.

For the microfluidic experiments, the channels were placed on the stage of an inverted microscope (IX71, Olympus, Japan) and the temperature of the stage was adjusted by means of a thermo plate controller (Tokai Hit, Japan) to 37°C. The flow rate of the working fluids was controlled using a syringe pump (KD Scientific Inc., USA), and two different flow rates were examined: 9.45 μL/min and 66.15 μL/min. The images of the flowing RBCs were captured using a high speed camera (Phantom v7.1, Vision Research, USA) and transferred to the computer to be analyzed. An illustration of the experimental set-up is shown in Fig. 2.

2.2 *Image analysis*

The original data obtained from the experiments are the digital video sequences captured at the frame rate of 4800 frames/s with the exposure time of 2 μs. This corresponds to the frame intervals of 208 μs. For the image analysis, firstly, the captured videos were converted to a sequence of static images (stack), with a resolution of 800 × 600 pixels each.

Then, in order to reduce the dust and static artifacts in the images, an averaged background image was created from the original images and subtracted from the stack. This process eliminates all the static objects from the images including the microchannel walls, which resulted in images having only the flowing RBCs visible. To enhance the image quality, image

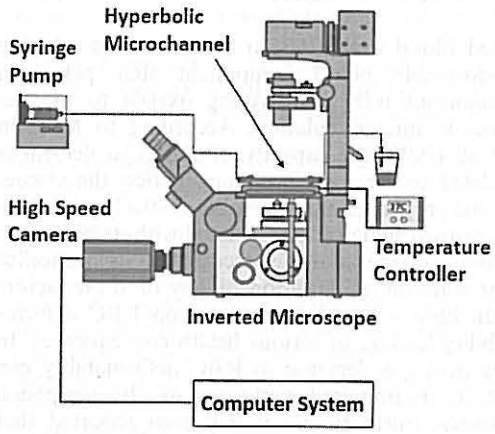

Figure 2. Experimental set-up.

filtering such as *Median* operation with the mask size of 3 × 3 pixels and *Brightness/Contrast* adjustment was applied using ImageJ (NIH). Finally, the grey scale images were converted to binary images adjusting the threshold level. ImageJ default threshold method based on IsoData method was applied first and then the level was adjusted manually for the optimal binarization. For instance, the ImageJ default threshold set the min. value as 0 and the max. value as 68 automatically for the images of flow rate 9.45 μL/min, but the max. value was slightly raised to 70 manually in order to obtain better binary images to analyze. This means the pixels with intensity levels in the range of 0–70 were set to be 0 (black) and the pixels with intensity levels greater than 70 were set to be 255 (white). This segmentation process yields regions of interest with RBCs as black circular objects (with or without holes inside) against a white background. More details about the intensity levels of the RBCs are described in Section 3.2.

To analyze the deformation index, the cells were measured in two pre-defined regions, (A) and (B) as shown in Fig. 1. Region (A) is located upstream of the hyperbolic contraction and region (B) comprises a narrow part of the contraction region. Both regions are located axially along the centerline of the channel.

The flowing cells selected for measurement in region (A) were tracked and identified in region (B). In other words, the same cells were measured twice, once in region (A) and another in region (B) in order to examine the DI transition of identical cells.

The *Analyze Particles* function in ImageJ (NIH) was used for measuring the cells dimensions. This command counts and measures objects in binary images according to the pre-defined measurement settings (e.g. centroid, width, length, etc.). Some parameters such as *Area* and *Circularity* are useful to ignore out-of-interest objects. In the current work, the area of the objects was limited to 17–50 μm² and the circularity to 0.5–1.0. These settings reasonably ignore the apparent deviant objects such as out-of-focus cells, aggregated cells, and so on.

Finally, the RBC deformation was characterized by the deformation index (DI) as $(A_{Major} - A_{Minor})/(A_{Major} + A_{Minor})$, where A_{Major} and A_{Minor} refer to the major (primary) and minor (secondary) axis lengths of the ellipse best fitted to the cell. These values were obtained by the measurements obtained with *Analyze Particles* operation.

3 RESULTS AND DISCUSSION

3.1 *Deformation index*

Fig. 3 shows RBCs flowing through the PDMS hyperbolic microchannel in original images at

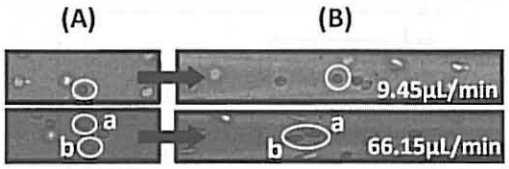

Figure 3. RBC deformation at different flow rates in region A and B.

different flow rates (9.45 μl/min and 66.15 μl/min) and in two pre-defined regions, (A) and (B). In Fig. 4 the average deformation index calculated based on the results of image analysis are shown for each case.

As can be seen in Fig. 4, for both flow rates, DI is higher in the hyperbolic contraction region (B) where the RBCs are submitted to a strong extensional flow. In the contraction region (B), DI increases substantially with the flow rate as a consequence of the higher strain rate to which the RBCs are submitted. These results evidence the highly deformable nature of RBCs under strong extensional flows.

3.2 *Intensity levels*

The images captured by a microscope with a high speed camera display RBCs with various light intensity levels (Fig. 5 (a)). When these are converted to binary images, they appear with rather different shape/size (Fig. 5 (b)). In this study, we distinguished RBCs by three levels of light intensity, corresponding to low (black), intermediate (grey) and high intensity (white), and the average deformation index was calculated for each class of RBCs. However, the results in Fig. 4 show only the low and intermediate intensity levels RBCs, as high intensity level cells were deemed to be out of focus for DI to be accurately determined—the different shape of the white cells can be clearly seen in Fig. 5 (b).

In Fig. 4 it is clear, that despite the shape of the grey cells being slightly more elongated than black cells, the differences are not very significant.

Additionally, we have quantified the flow velocities of the cells considering their intensity level. Fig. 6 presents our preliminary results of the cell flow velocities for the two intensity level groups considered for DI measurements: low intensity cells (black cells) and intermediate intensity cells (grey cells). As expected, the velocity increases as the cells travel through the hyperbolic microchannel at its centerline. Additionally, the velocities of intermediate intensity cells are higher than those of the low intensity cells. This result may be related to the fact that we are using

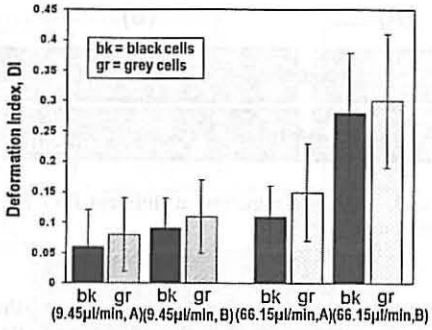

Figure 4. Comparison of deformation index at different flow rates in different regions.

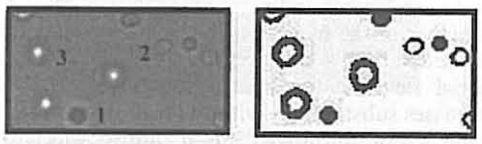

Figure 5. (a) Original image containing RBCs with various intensities: 1. low (black), 2. intermediate (grey) and 3. high (white), and (b) Corresponding binary image.

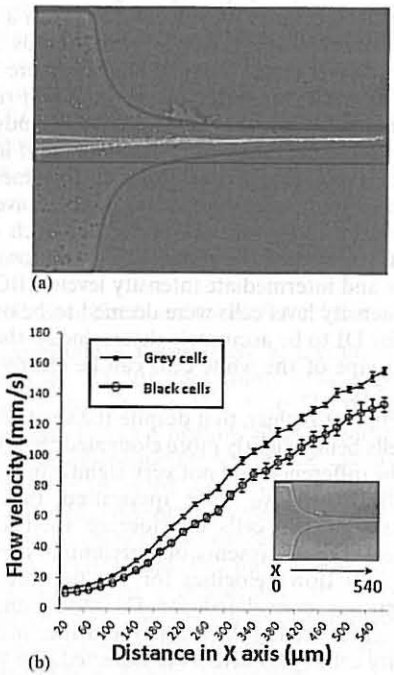

Figure 6. (a) Tracking of RBCs with different intensity levels for velocity measurements. (b) Axial velocity profiles of the low and intermediate intensity RBCs along the centerline at $Q = 9.45$ µl/min.

volume illumination, in which the depth-of-focus is determined by the characteristics of objective used. As a consequence, despite being centered at the mid-plane of the channel where the cell velocity is the highest, cells at different z-planes are also captured. In this case, we believe that the black cells are not truly located at the mid-plane and therefore its velocity is slightly lower than that of the grey cells. Following these preliminary results, further investigation on the cell velocities and deformation index in various regions of the microchannels under different flow conditions will be performed.

ACKNOWLEDGEMENTS

We thank Dr. Matsuki for help with blood sample collection. Additionally, we acknowledge the financial support provided by 2007 GlobalCOE Program "Global Nano-BME Education and Research Network", Japan. We are also thankful to FCT (Portugal) and COMPETE for financial support through projects PTDC/SAU-BEB/108728/2008, PTDC/SAU-BEB/105650/2008 and PTDC/EME-MFE/099109/2008.

REFERENCES

Abramoff, M., Magelhaes, P., Ram, S., 2004. Image processing with image. J. Biophotonics Int. 11, 36–42.

Dobbe, J.G.G., Hardeman, M.R., Streekstra, G.J., Strackee, J., Ince, C., Grimbergen, C.A., 2002. Analyzing red blood cell-deformability distributions. Blood Cells, Mol. Dis. 28, 373–384.

Fujiwara, H., Ishikawa, T. Lima, R., Matsuki, N., Imai, Y., Kaji, H., Nishizawa, M., Yamaguchi, T., 2009. Red blood cell motions in a high hematocrit blood flowing through a stenosed micro-channel. J. Biomech. 42, 838–843.

Gueguen, M., Bidet, J.M., Durand, F., Driss, F., Joffre, A., Genetet, B., 1984. Filtration pressure and red blood cell deformability: evaluation of a new device: erythrometre. Biorheology Suppl. 1, 261–265.

Mokken, F.Ch., Kedaria, M., Henny, Ch.P., Hardeman. M.R., Gelb, A.W., 1992. The clinical importance of erythrocyte deformability, a hemorrheological parameter, Ann. Hematol. 64, 113–122.

Oliveira, M.S.N., Alves, M.A., Pinho, F.T., McKinley, G.H., 2007. Viscous flow through microfabricated hyperbolic contractions. Exp. Fluids. 43, 437–451.

Shelby, J.P., White, J., Ganesan, K., Rathod, P.K., Chiu, D.T., 2003. A microfluidic model for single-cell capillary obstruction by Plasmodium falciparum-infected erythrocytes. PNAS. 100, 14618–14622.

Shin, S., Ku, Y., Park, M.S., Suh, J.S., 2004. Measurement of red cell deformability and whole blood viscosity using laser-diffraction slit rheometer. Korea-Australia Rheol. J. 16, 85–90.